

# H I L G A R D I A

*A Journal of Agricultural Science Published by  
the California Agricultural Experiment Station*

VOL. 31

NOVEMBER, 1961

No. 11

## **PREDICTED AND EXPERIMENTAL WATER TABLE DRAWDOWN DURING TILE DRAINAGE<sup>1</sup>**

**WILFRIED BRUTSAERT,<sup>2</sup> GEORGE S. TAYLOR,<sup>3</sup> and JAMES N. LUTHIN<sup>4</sup>**

### **INTRODUCTION**

The design of a drainage system must be based on sound physical principles. Information which increases understanding of the drainage process is the basis for the development of a rational system of drainage design.

The past few years have produced a vast amount of literature on the subject of drainage. Both theoretical and experimental results have been reported. Much progress has been made in the development of rational criteria for the design of drainage systems. However, there is still much to be learned, especially with regard to the non-steady state situation of a moving water table.

The present study describes some of the factors that are important during tile drainage and that affect the shape and the positions of a falling water table. The study describes successive positions of a falling water table as a series of steady states and is inspired by an analogous method used by Kirkham and Gaskell (1951).<sup>5</sup> The main difference is that here a capillary fringe and a changing drained porosity are taken into account. The results of the theoretical analysis are compared with experimental results obtained by Luthin and Worstell (1957).

Evaluations of the potential distribution in the draining soil profile were obtained with an electrical resistance network. To check theoretical results with experimental data, the network was set up in the same dimensions as the sand tank in the experimental study of Luthin and Worstell (1957).

<sup>1</sup> Submitted for publication August 4, 1960.

<sup>2</sup> Research Assistant, Department of Irrigation, Davis.

<sup>3</sup> Formerly Visiting Associate Professor (Ohio State University), Department of Irrigation, Davis.

<sup>4</sup> Professor, Department of Irrigation, Davis.

<sup>5</sup> See "Literature Cited" for citations referred to in the text by author and date.

## PREVIOUS WORK

An exact solution for the case of the falling water table is difficult because of the non-steady state conditions of this phenomenon. Non-steady state flow is said to occur when the velocity at any point of a flow system changes with time. Many investigators, including Spöttle (1911), Walker (1952), Visser (1953) and Glover (Dumm, 1954) attempted to derive analytical solutions. These solutions are based on simplifying assumptions, and their validity may be questioned. Recently, Luthin (1959) proposed a non-steady state drainage formula which is based on empirical assumptions.

Childs (1947) approached the non-steady drainage problem by considering a series of successive steady-state water table positions. Using an electrical analogue method, he found each position of the water table by trial and error. An initial water table shape, ponded or in equilibrium with a steady rainfall, must first be determined. After cessation of rain the next position of the falling water table is found. A trial and error procedure is necessary because of two conditions which must be satisfied: the voltage applied at a point corresponding to the upper boundary of the capillary fringe is proportional to the hydraulic potential; and the current input at the same point is proportional to the water table drop

As reported by Childs (1947), the algebraic expression of the first condition is:

$$V = Ah - C \quad (1)$$

where  $V$  is the electrical potential,  $h$  is the height of the point considered above the drain, and  $A$  and  $C$  are constants which are the analogues of the quantities  $g\rho$  and  $p_c$  in the equation:

$$\phi = g\rho h - p_c \quad (2)$$

Equation (2) is the well known Bernoulli equation in which the velocity potential is neglected,  $\phi$  is the hydraulic potential,  $g$  the acceleration due to gravity,  $\rho$  the density of water, and  $p_c$  the pressure at which the upper limit of the capillary fringe is defined. The capillary fringe is called the zone of soil just above the water table which is still essentially saturated although under suction.

The second condition is:

$$i_d = K\Delta h_d \quad (3)$$

where  $i_d$  is the current input in the analogue per unit length of fringe boundary at a horizontal distance  $d$  from the drain ordinate,  $K$  is a constant, and  $\Delta h_d$  is the distance the water table falls. The derivation of equation (3) is straightforward if  $\Delta h_d$  is small enough so that  $dh/dt = \Delta h/\Delta t$ , and if  $\Delta t$  and  $(c_s - c_u)$ , ( $c_s$  and  $c_u$  are the moisture content of the soil in the saturated and

the unsaturated phase respectively) are constant over the distance of fall  $\Delta h$  in the following equation:

$$\psi_d = - (c_s - c_u) \left( \frac{dh}{dt} \right) \quad (4)$$

where  $\psi_d$  is the fluid flux across the fringe boundary at point  $d$ , and  $dh/dt$  is the vertical rate of fall of the water table.

As will be shown later, the assumption that  $(c_s - c_u)$  is a constant is a deviation from the true physical phenomenon. It is physically impossible that the soil drains all its water at once when the upper boundary of the capillary fringe passes a given point. Because of the resistance to flow, the suctions which cause the water to be removed from the soil increase only gradually as drainage proceeds.

The shapes of the water tables reported by Childs (1947) show a remarkable flatness and seem to agree with the experimental data of Luthin and Worstell (1957). On the other hand, Kirkham and Gaskell (1951), using the same assumption in a similar numerical method, obtained curvilinear rather than flat water tables. A possible explanation for this difference in shape is that Childs had compensating errors in his assumptions and that Kirkham and Gaskell did not. In Childs' work the assumption that  $(c_s - c_u)$  is a constant is probably cancelled by the assumption that the distance over which the capillary fringe falls is proportional to the current input. According to Kirkham and Gaskell (1951) the latter assumption may be corrected by saying that the vertical distance of fall is proportional only to the vertical component of the current at the top of the capillary fringe. The fact that Childs does not take this refinement into consideration probably results in a horizontal water table. Even though Childs' assumptions may not be entirely correct, his work gave a good insight into the non-steady state drainage problem. Until Childs' work the non-steady case had too often been simplified to one of a steady state.

As mentioned before, Kirkham and Gaskell (1951) derived the positions and shapes of a falling water table in essentially the same way as Childs, namely by a series of steady state flow conditions. The potential distribution in the soil profile for an initially known water table position is found by a numerical solution of Laplace's equation based on a relaxation procedure. The next water table position is then determined, not by trial and error as in Childs' method, but by a simple formula based on Darcy's law. One weakness of the method is the assumption that the pores are essentially drained at once as the water table recedes and, consequently, that no flow occurs above the water table. This assumption probably accounts for the difference in shape of the water table positions obtained in the experiments of Luthin and Worstell (1957) and those calculated by Kirkham and Gaskell.

Since the Kirkham and Gaskell equation is used for further mathematical derivations, its derivation is now given in detail. In figure 1 an infinitely

small portion of the water table  $AB$  is allowed to fall along the streamlines  $AC$  and  $BD$ . Let  $\theta$  be the slope of the water table and  $\beta$  the angle between the streamlines and the vertical, then it follows that the vertical component of the distance of water table fall  $AE$  is given by:

$$AE = AC (\cos \beta - \sin \beta \tan \theta) \quad (5)$$

According to Darcy's law the total distance of fall  $AC$  during time  $T$  is equal to:

$$AC = TK \frac{\partial \phi / \partial s}{f} \quad (6)$$

where  $K$  is the hydraulic conductivity,  $f$  is the fraction of the soil which is occupied by drainable water, and  $(\partial \phi / \partial s)$  is the partial derivative of the hydraulic potential with respect to path length along  $AC$ . Substituting equation (6) in (5) results in:

$$AE = \frac{TK}{f} \left( \frac{\partial \phi}{\partial s} \right) (\cos \beta - \sin \beta \tan \theta) \quad (7)$$

Using

$$\frac{\partial \phi}{\partial s} \cos \beta = \frac{\partial \phi}{\partial y} = \phi_y \quad \text{and} \quad \frac{\partial \phi}{\partial s} \sin \beta = \frac{\partial \phi}{\partial x} = \phi_x$$

in equation (7) yields the final equation:

$$AE = \frac{TK}{f} (\phi_y - \phi_x \tan \theta) \quad (8)$$

The main difference between the above analysis and that of Childs is the factor  $(\phi_y - \phi_x \tan \theta)$  as used in equation (8), and not simply  $\phi_s$  which is proportional to the factor  $i_d$  of Childs.

The main objective of the present study is to modify the Kirkham and Gaskell analysis by introducing a capillary fringe and also a porosity factor which is dependent upon water table depth. Two additional objectives are:

1. Adaptation of the electrical resistance network to yield the components of the potential gradient  $\phi_y$  and  $\phi_x$  during water table drawdown, and
2. Comparison of an analysis of the falling water table as a succession of steady states with experimental results of Luthin and Worstell (1957).

## PHYSICAL AND MATHEMATICAL THEORY OF THE FALLING WATER TABLE

### Analysis of the Experimental Study by Luthin and Worstell

**Tank and Soil.** The experimental results of Luthin and Worstell (1957) will be compared with the water tables predicted by the physical analysis developed in this section. The completeness of their experimental results makes their findings suitable for the comparison.

The inside dimensions of the tank, as described by Luthin and Worstell, were 6 feet high, 10 feet long and 2 feet wide. A 3-inch diameter tile drain was at one end of the tank, 1.5 feet above the bottom. In this way a tile spacing of 20 feet was simulated with the soil surface approximately 3.75 feet above the tile line and the impervious layer 1.50 feet below it.

The tank was filled with a fine sand obtained from dunes near Oso Flaco, California. It has a well defined capillary fringe of about 23 cm or 0.75 foot. The maximum drainable porosity is about  $0.35 \text{ cm}^3/\text{cm}^3$ , which can be observed from the moisture characteristic curve A, in figure 2. This curve, which is obtained from data given by Day and Luthin (1956) and by Luthin and Worstell (1957) is defined in this study as the soil moisture-suction curve. The saturated hydraulic conductivity  $k$  of Oso Flaco sand is about 48 feet/day or 0.0334 feet/minute.

**Soil Moisture-Water Table Depth Relationship.** In a draining soil it is not clear how the moisture content at a point and the water-table depth are related. If the suction of the water at this point were equal in magnitude to the height of the point above the water table, the soil moisture-suction curve A of figure 2 would represent this relationship.

According to the soil column study by Luthin and Miller (1953) however, the depth of the water table does not equal the actual suction. They point out that as soon as the water disappears from the soil surface, the water table drops almost instantaneously to the bottom of the column. At this time the soil is still saturated and the tensiometers at all depths read only small values. These suctions increase with height in the column but always remain lower than the actual height above the water table. As drainage proceeds the readings become higher. It is only when equilibrium is reached, i.e. when the column stops draining, that the suction at any point in the column becomes equal to the height of this point above the water table. Under these static conditions the moisture profile in the soil and the moisture-suction curve are equivalent. As the drainage phenomenon in the tank is definitely dynamic, the drained porosity is not represented by the static moisture-suction curve. Hence another relationship must be utilized.

The average drained porosity between the  $(n - 1)$ -th and the  $n$ -th position of the water table is defined as:

$$f_a = w'/(y_n - y_{n-1}) \quad (9)$$

where  $w'$  is the water drained from the soil between the stable water table positions ( $\text{cm}^3$  of water per  $\text{cm}^2$  of soil surface) and where  $y_n$  and  $y_{n-1}$  are the average depths of the water table below the soil surface at the  $n$ -th and the  $(n - 1)$ -th position, respectively.

If the water table be falling very slowly, as in the case of wide tile spacings, the soil moisture profile above the water table would be given quite clearly by the moisture suction curve. Under these conditions and for a homogeneous soil the drain outflow water  $w'$  may be assumed to come from a soil

portion of thickness  $y_n - y_{n-1}$  having an average water film tension given by  $(y_n + y_{n-1})/2$ .

In the model tank with narrow tile spacing, however, the water table falls relatively fast. It is incorrect to assume that water drains only from a layer of thickness  $y_n - y_{n-1}$ . Actually, water is being drained from all parts of the soil profile in response to gradients whose magnitudes are not exactly known owing to the dynamic situation. Therefore, in this study the porosity factor defined by the water table depth will be called the "apparent" drained porosity because the water is assumed to come from a layer thickness  $y_n - y_{n-1}$ . Hence the apparent drained porosity is given by:

$$f_a' = w/(y_n - y_{n-1}) \quad (10)$$

where  $w$  is the water drained from the entire soil profile above the water table when the water table falls from the  $(n - 1)$ -th to the  $n$ -th position. An experimental curve relating  $f_a'$  and water table depth  $y$  can be obtained by plotting  $f_a'$  against  $(y_n + y_{n-1})/2$ .

For example, the total water drained from the experimental tank in the time interval from 2 to 8 minutes may be calculated by measuring the area under the curve and between vertical lines at 2 and 8 minutes in figure 4. (16,800 cm<sup>3</sup>). For a tank of 61 cm width and 300 cm length the water drained is equivalent to 0.917 cm of ponded water. During the same time, an apparent soil volume of 6,450 cm<sup>3</sup>/cm tank width has been drained or  $y_n - y_{n-1} = 6,450$  cm<sup>2</sup>/300 cm or 21.5 cm. This gives then the apparent drained porosity  $f_a' = 0.917$  cm/21.5 cm or 0.0427. In figure 3 it is also seen that the average depth of the water table between 2 and 8 minutes is about 40 cm (or about 80 cm above the tile drain). In this manner a plot of the apparent drained porosity as a function of the water table depth was obtained and is shown in figure 5. From 0 to 23 cm ( $\frac{3}{4}$  foot) an initial horizontal line represents the capillary fringe. Greater water table depths result in a linear increase in the drained porosity function. This curve will be referred to hereafter as the soil moisture-water table depth relationship.

It must be emphasized that the curve of figure 5 holds for only this particular drainage problem. For example, different tile spacings in the same soil might give a different soil moisture-water table depth relationship. Consider the extreme case where the spacing is zero, which is in fact a column as studied by Luthin and Miller (1953). Here the water table falls almost instantaneously and the  $y$  values are initially higher than the suction. In the other extreme case where the spacing is infinite, the water table does not fall at all. In other words the soil moisture profile is in equilibrium and the moisture conditions above the water table are equivalent with the moisture-suction curve. It may therefore be expected that with larger tile spacings the moisture-water table depth curve will more closely approximate the moisture-suction curve A in figure 2.

## Mathematical Equations for the Rate of Fall of the Water Table

**Effect of the Capillary Fringe.** The soil moisture-suction curve A of figure 2 shows that the suction in the soil has to reach a critical value  $y_c$  before an appreciable amount of water is drained. Consequently, there is a zone of substantial thickness above the water table which is nearly saturated. This zone, defined earlier as the capillary fringe, undoubtedly has a conductivity nearly as high as the zone below the water table and therefore cannot be neglected in evaluating moisture flow. Because almost no water drains as long as the suction is lower than the above-mentioned critical value  $y_c$ , a water table initially at the soil surface may be assumed to fall almost instantaneously until it reaches a depth for which the suction at the soil surface is approximately  $y_c$ .

In calculating water table drawdown, the position of the upper boundary of the capillary fringe will be predicted rather than the water table. For convenience in subsequent calculations, the ordinate of figure 5 is translated 23 cm to the right. The abscissa title is changed accordingly to read "depth of the upper boundary of the capillary fringe" instead of "depth of the water table." The apparent drained porosity is then everywhere linearly related to the depth of the upper capillary fringe boundary with the same slope  $a$  as shown in figure 5. Thus  $f'$  is given by equation (11), where  $y'$  now represents the distance from the soil surface to the upper fringe boundary.

$$f' = ay' \quad (11)$$

After the position of the upper fringe boundary and the potential distribution in the soil profile are determined, the position of the water table is easily ascertained. The water table is represented by the locus of points at atmospheric pressure or the locus of points at which the potential is equal to the height above the tile line.

**Linear Relationship.** The drawdown equation of Kirkham and Gaskell (8) will now be modified for the case when the porosity is linearly related to the depth of the upper capillary fringe boundary. It is this relation, expressed in equation (11), which is used to calculate the amount of water drained as a result of the falling water table. Consider that the upper capillary fringe boundary falls over an infinitely small distance  $dy'$  and that a quantity of water  $dw$  drains from the soil profile above the fringe boundary so that:

$$dw = f' dy' \quad (12)$$

Using the linear relation  $f'$  of equation (11) in the above equation gives:

$$dw = ay' dy'$$

By integration between  $y'_{n-1}$  and  $y'_n$  the total water drained is calculated.

$$w = \int_{y'_{n-1}}^{y'_n} ay' dy' = \frac{a}{2} (y_n'^2 - y_{n-1}'^2) \quad (13)$$

If equation (12) is integrated by taking  $f'$  as a constant average value  $f'_a$  between average positions  $y'_{n-1}$  and  $y'_n$ , the equivalent of equation (10) is obtained. The amount of water  $w$  that flows out of the drain also passes through the upper boundary of the capillary fringe, therefore the apparent drained porosity  $f'_a$  is the same as the drainable pore space  $f$  used by Kirkham and Gaskell. By replacing  $f$  in equation (8) by  $f'_a$  and substituting  $AE$  with  $(y'_n - y'_{n-1})$ , the following equation is derived from the equivalent of equation (10):

$$w = Tk \phi_e \quad (14)$$

where  $\phi_e$  represents  $(\phi_y - \phi_x \tan \theta)$ . Upon substituting equation (14) in (13) the  $n$ -th position of the upper capillary fringe boundary is:

$$y'_n = \left( \frac{2Tk \phi_e}{a} + y_{n-1}'^2 \right)^{1/2} \quad (15)$$

Equation (15) was used in this study to calculate the drawdown in a drainage system with the same dimensions as the tank of Luthin and Worstell.

**Transition from Linear Relationship to Constant Drained Porosity.** As explained earlier, the moisture-suction curve may be applicable in the case of wide tile spacings. Curve A in figure 2 indicates that above 53 cm, the drained porosity remains approximately constant at 35 per cent by volume. This means that at a drained porosity of 0.35, drainage virtually ceases. For convenience of calculation, curve B of figure 2, which approximates curve A, has also to be translated. As with figure 5, the ordinate is translated 23 cm to the right and the abscissa title changed to read "depth of the upper boundary of the capillary fringe below the soil surface" instead of "suction".

Equation (15) is applicable only for the sloping part of this translated moisture-suction curve. For the example shown in figure 2, the depth of the upper boundary of the capillary fringe must be smaller than 30 cm, namely (53 - 23) cm. For greater depths, the Kirkham and Gaskell formula can be used without error because then the drained porosity remains almost constant. For the case, however, where the top of the capillary fringe falls from  $y'_{n-1}$  to  $y'_n$  and where  $y'_{n-1} < 30 \text{ cm} < y'_n$ , a new relation must be found. After translation of curve B in figure 2,  $dw = ay' dy'$  from  $y' = y'_{n-1}$  to  $y' = y'_i$  ( $y'_i = 30 \text{ cm}$ ), and  $dw = f_i dy'$  from  $y' = y'_i$  to  $y' = y'_n$ , where  $f_i$  is the constant drainable pore space 0.35. After integration the volume of drained water is given by:

$$\begin{aligned} w &= \int_{y'_{n-1}}^{y'_i} ay' dy' + \int_{y'_i}^{y'_n} f_i dy' \\ &= \frac{a}{2} (y_i'^2 - y_{n-1}'^2) + f_i (y'_n - y'_i) \end{aligned} \quad (16)$$

If the water table depth is equal to the suction, substitution of equation (14) in (16) gives the  $n$ -th position of the upper capillary fringe boundary:

$$y'_n = \frac{Tk \phi_e}{f_i} - \frac{ay_1'^2}{2f_i} + y'_1 + \frac{a}{2f_i} y_{n-1}'^2 \quad (17)$$

**Broken Line Relationship.** It is also possible to approximate the moisture-tension curve more closely by a series of connected straight lines. An equation similar to (15) and (17) may then be obtained.<sup>6</sup> However, the numerical complications involved do not seem to justify this refinement.

## EXPERIMENTAL PROCEDURE

### Adaptation of the Electrical Network to a Specific Drainage Problem

A fast way of solving steady two-dimensional flow problems is to simulate the flow medium by a network of electrical resistors. This method, proposed by Luthin (1953) to solve drainage problems, was used in the present study to find the potential distribution in the soil profile. From the potential distribution, the gradients at the upper boundary of the capillary fringe needed to solve equation (15) were obtained.

The network was set up according to the specifications of Worstell and Luthin (1959). One-fourth watt carbon resistors soldered inside glass cartridge type "fuses" were plugged into clips mounted on plastic panels in a grid pattern to form the network. The network was assembled to simulate the tank dimensions as reported by Luthin and Worstell (1957). The basic network resistor was 10 megohms. Because large changes in potential occur directly above and close to the drain, a finer mesh was used in this region. Therefore, the first 3 feet away from the drain were simulated by a mesh of 10 megohms per 3 inches. The other 7 feet were simulated by a mesh of 10 megohms per 6 inches. The boundary conditions were fixed according to the principles given by Luthin (1953). On the impervious boundaries the resistance of the resistors was 20 megohms.

Two resistors were frequently connected in parallel or series to obtain the desired values at the top of the capillary fringe. Because the radius of the tank drain was 1.5 inches the resistance of the adjacent resistors had to be 5 megohms in the horizontal direction and 10 megohms in the vertical direction on the line of symmetry through the drain.

An ordinary 24-volt battery served as potential source necessary to operate the network. The desired voltages at the top of the capillary fringe were obtained with 0.5 megohm rheostats.

With the upper edge of the tile as reference the potential of the capillary fringe boundary is:

$$\phi_e = h_e - y_e - r_d \quad (18)$$

<sup>6</sup> Brutsaert, Wilfried. Unpublished MS thesis, Graduate Division of the University of California.

where  $h_c$  is the height of the capillary fringe above the center of the drain,  $y_c$  is the maximum tension at which the soil is still saturated, and  $r_d$  is the radius of the drain. One foot of hydraulic potential was represented by  $n$  volts of electrical potential. Written in electrical units, equation (18) becomes:

$$V_c = n(h_c - y_c - r_d) \quad (19)$$

where  $V_c$  is the voltage to be applied at the upper boundary of the capillary fringe. To have the potential gradients at the top of the capillary fringe,  $\phi_y$  and  $\phi_x$  in feet per foot, the voltage differences were measured over a finite distance of 3 inches. The total current outflow was obtained by determining the voltage across a known resistor in series with the drain electrode. The electrical current units must be converted to hydraulic rate of flow units.

From Darcy's law,

$$v = k \frac{\partial \phi}{\partial s} = \frac{k}{n} \frac{\partial V}{\partial s},$$

and from Ohm's law

$$i_0 = \frac{1}{R_0} \frac{\partial V}{\partial s}.$$

The outflow conversion formula is therefore:

$$q = \frac{k}{n} R_0 i \quad (20)$$

where  $q$  is the outflow per unit drain length in cubic feet of water per minute,  $n$  the conversion factor from volts to feet,  $k$  the hydraulic conductivity in feet per minute,  $R_0$  the basic network resistance and  $i$  the electrical current in amperes. As  $n = 4$ ,  $k = 48$  feet/day and  $R_0 = 10 \times 10^6$  ohms, equation (20) becomes:

$$q = 0.0834 \times 10^6 i \text{ (in cfm)} \quad (21)$$

Because the currents in the network were very low, a high resistance vacuum tube voltmeter was necessary to measure the potentials. The network is shown in figure 6 for a particular position of the water table.

Because this study is essentially the approximation of a non-steady flow problem by a series of steady state conditions, an initial position must be known. The easiest position to determine is the ponded water table, from which the subsequent positions may be calculated one after the other. The steps followed in this procedure are:

1. Assembly and adjustment of the network for a particular boundary condition.
2. Voltage measurements within the network.
3. Computation of the next position of the fringe with equation (15) and repetition of steps 1 through 3.

## RESULTS AND DISCUSSION

**Results.** The different positions of the upper fringe boundary and the corresponding positions of the water table which were obtained with the method described in this study are designated by the numbers 0 through 7. Position 0 represents the water table at the surface of the soil (see figure 7). Position 1 represents the completely saturated soil profile when the upper fringe boundary is at the soil surface. The water table is assumed to fall instantaneously from position 0 to 1. Thus it can be seen from the shapes of the equipotential lines in figures 9 to 13 that, as the water table falls, the flow changes gradually from radial to essentially horizontal in direction. So for the low water table shown in figure 13, the flow pattern approximates the Dupuit-Forchheimer idealization (Muskat, 1946). When the water table approaches the drain as shown in figure 13 the potential differences are quite small and cannot be measured accurately. Therefore position 7 was not set up in the network, but only calculated from position 6. In the initial positions the capillary fringe is thicker than for the later positions, especially over the drain. In position 1, (figure 8) the capillary fringe has a maximum thickness of about 1.25 foot. As the water table approaches drain depth, the fringe is approximately 0.75 foot (see figure 13).

The vertical and the horizontal components of the potential gradients at the upper capillary fringe boundary,  $\phi_y$  and  $\phi_x$  are plotted in figures 14 and 15. For initial positions as shown in figure 14, the  $\phi_y$  values are maximum directly over the drain ( $x = 0$ ) and minimum at the midpoint between drains ( $x = 10$  feet). Directly over the drain these values decrease as the water table recedes until finally (position 6) they become smaller than those at the midpoint. At the midpoint  $\phi_y$  stays almost constant. The horizontal components of the potential gradient at the upper capillary fringe boundary are given in figure 15 for positions 3 to 6. The first three positions (0, 1, 2) are not considered since  $\phi_x$  is quite small compared with the  $\phi_y$  values. The  $\phi_x$  values shown in figure 15 are zero immediately above the drain and at the midpoint. Elsewhere along the fringe boundary they increase with each water table drop and reach a maximum value for position 6. Figure 16 shows the product  $\phi_x \tan \theta$  for the different positions of the upper capillary fringe boundary. These values are much smaller than either the  $\phi_y$  and the  $\phi_x$  values. However, their curves are of the same general shape as those of  $\phi_x$ . The value of  $\phi_y$  and the product  $\phi_x \tan \theta$  were used in equation (15) for the calculation of the water table at times corresponding to those at which positions 1 through 7 were obtained.

Calculated positions of the water table for corresponding times are presented in figure 17. For initial positions the water table shapes are essentially flat. The water table of position 4 has the greatest curvature. As the water table reaches drain depth, its shape is again almost horizontal. The interpolated values of the above water table positions are in agreement with those obtained by Luthin and Worstell (figure 18) with respect to both shape and

drawdown time. The shapes obtained in the network show slightly greater curvature than those from the sand tank study. Except for an initial discrepancy at 2 minutes, the times agree quite closely.

In figure 19 the drain outflow rate, as calculated from the electrical resistance network data, is compared with the drain outflow from the tank model. Under ponded conditions, the network and the tank both indicated a rate of flow of 4.25 liters per minute. In the network the rate of flow dropped instantaneously to 3.20 liters per minute when the ponded water disappeared from the soil surface, while in the tank the decrease was not as large. Later the time lag between the curves was of the order of 2 to 3 minutes or 0.2 liters per minute. This lag became more pronounced at lower rates of flow.

The relationship between the height of the water table at the midpoint and the drain outflow is seen to be linear in figure 20. It is in agreement with Luthin's first assumption used in the derivation of his drainage formula (Luthin 1959).

### General Discussion

It can be seen from figures 7 to 13 that the flow pattern in the soil profile becomes nearly horizontal as the water table recedes. This phenomenon is also indicated by the fact that the  $\phi_y$  values decrease and the  $\phi_x$  values increase when the water table approaches drain depth. In other words, the potential gradients become larger in the horizontal direction and smaller in the vertical. This is largely due to the shallow depth of the impervious layer.

Directly over the drain, the  $\phi_y$  values are maximum because the path to be followed by a water particle is shorter at this place than further away from the drain. As  $\phi_x \tan \theta$  is always zero directly above the drain, the factor  $(\phi_y - \phi_x \tan \theta)$  is maximum at  $x = 0$ . Therefore the water table initially falls the fastest over the drain. Because of this fast initial rate of fall the hydraulic head above the drain drops rapidly and even though the path length is still short the  $\phi_y$  values decrease quite considerably. At the midpoint the  $\phi_y$  values stay nearly constant because the hydraulic head and the length of the streamlines decrease in the same proportion. The main effect of decreasing values of  $\phi_y$  at  $x = 0$  is that the water table assumes a horizontal shape as it approaches drain depth.

The  $\phi_x$  and the  $\phi_x \tan \theta$  values directly over the drain and at the midpoint are zero. These conditions exist because no horizontal flow can take place across the vertical symmetry planes through the center of the drain and at the midpoint. As the water table falls, the region of flow becomes smaller and smaller. Therefore the average value  $\phi_x$  increases and the flow becomes more horizontal in direction. The shapes of the capillary fringe boundary for position 0 through 7 do not differ much and consequently, the  $\tan \theta$  values also do not change materially. Therefore the curves of  $\phi_x \tan \theta$  have the same general shape as those for  $\phi_x$ . The magnitude of  $\phi_x \tan \theta$  remains small compared with  $\phi_y$ . This means that  $\phi_y$  of equation (15) is the main factor in determining the rate of fall of the upper capillary fringe boundary and is almost equal to  $\phi_e$  (see equation 15) in the beginning.

The behavior of the capillary fringe during the recession is due to the fact that the flow conditions change from dynamic in the beginning to nearly static when the water table approaches the drain. Actually the phenomenon is closely related to the change in potential gradient at the upper capillary fringe boundary. As discussed previously, the gradient is maximum in the beginning, especially directly over the drain. Therefore, in accordance with the theory on page 394, a maximum lag may be expected between the suction and the height above the water table and hence also between the suction in the capillary fringe and its thickness. When at the end equilibrium is approached, the gradients also approach zero and the capillary fringe thickness of the final positions is equal to its tension, namely 0.75 foot.

The water tables obtained with the network are more curvilinear than those obtained by Luthin and Worstell. This is due to the fact that finite steps were taken (6 inches directly over the drain) instead of infinitesimally small increments. Therefore the  $\phi_u$  value right over the drain, which decreases from step to step, was used over too great a distance. This caused the upper capillary fringe boundary at that point to fall deeper, as compared with the midpoint, than it actually did in the sand tank. Another unknown but probably small error is introduced by neglect of the flow in the region above the capillary fringe.

From positions 3 to 7, the drawdown times as determined by the network and the sand tank agree. This substantiates the validity of the moisture-water table depth relationship in this range. The deviation in the initial positions is due to the approximation of the calculated points of the moisture-water table depth relationship (figure 5) by the simplified broken line curve. This approximation is based on the assumption that the capillary fringe is completely saturated. This is apparently not correct when the calculated points are considered.

The difference between the drain outflow rates obtained from electrical current data and those from the sand tank may be a result of the simplifying assumptions on which the present study was based. First of all, from the assumption that the capillary fringe is completely saturated, it follows directly that the water table drops instantaneously until the upper capillary fringe boundary is at the soil surface. The second simplifying assumption already mentioned above is that the whole drained soil profile was represented by a network in which the zone of flow above the upper capillary fringe boundary was neglected.

### Discussion of Other Methods

**Water Table Depth and Suction.** The difference between the water table depth and the suction has been discussed earlier. It was concluded that both are identical only under equilibrium conditions or when the tile spacings are relatively wide, such as in field installations. Therefore in the case of the tank the moisture-water table depth curve must be used in the drawdown formula instead of the moisture-suction curve.

Nevertheless, it is still interesting to investigate what the result would have been if the moisture-suction curve had been used. This has been done for the first four positions of the water table. In equation (15) it is only the slope  $a$  of the moisture-suction curve which will be different from the one of the moisture-water table depth curve. All the other factors remain the same; therefore, only the time interval  $T$  will be affected.

The factor  $a$  of the soil moisture-water table depth curve as used in the procedure discussed above is  $0.166 \text{ ft}^{-1}$  (figure 5). The factor  $a$  of the soil moisture-suction curve is about  $0.356 \text{ ft}^{-1}$  (figure 2). The positions of the upper capillary fringe boundary which are obtained by using the latter value of  $a$  are exactly the same as before; the times differ, however, proportionally with the factor  $a$  as is seen in the table below.

Position	Times of drainage (minutes)	
	$a = 0.166 \text{ ft}^{-1}$	$a = 0.356 \text{ ft}^{-1}$
1.....	0	0
2.....	1.5	3.23
3.....	6.5	13.88
4.....	16.15	29.88

It has been pointed out earlier that as tile spacings become wider, the moisture-suction curve probably approximates the moisture-water depth curve. On the other hand it is seen from the comparison in the table that the soil moisture-suction curve indicates slower drainage than actually occurs. In other words, if a field drainage problem is analyzed by using the soil moisture-suction curve, the obtained time intervals are too long. Hence the calculated spacings would be too narrow.

**Effect of the Capillary Fringe.** To determine the effect of the capillary fringe on water table drawdown, the analysis proposed in this study must be compared with one in which the capillary fringe is omitted. For this purpose the moisture-suction curve was approximated by a linear relationship  $C$  which starts at the origin as a straight line with a slope of  $a = 0.152 \text{ ft}^{-1}$  as shown in figure 2. The potential applied at the upper limit of the network, in this case the water table, was then:

$$V = 4 (h_w - r_d) \tag{22}$$

where  $h_w$  is the height of the water table above the center of the drain, and  $r_d$  the radius of the drain. The potential gradients  $\phi_v$  obtained just below the water table are given in figure 21. As only the initial positions are considered, the  $\phi_x \tan \theta$  values may be neglected.

The water table positions obtained by omitting the capillary fringe are shown in figure 22 and compared with those of figure 17. In fact these water table positions are the positions of the upper capillary fringe boundary of the figures 7 to 13. This comparison supports the objections that Luthin and Miller

(1953) made against the Kirkham and Gaskell method. It is seen in figure 22 that, as Luthin and Miller suggest, and as is done in the proposed analysis of this study, the term "water table" should be replaced by "upper boundary of the capillary fringe".

**Comparison with the Kirkham and Gaskell Analysis.** In the Kirkham-Gaskell equation (8) the drained porosity is assumed to be constant and the capillary fringe is neglected. In other words the soil at any point is supposedly drained at once when the water table passes by. The total drainable porosity of Oso Flaco sand is about 35 per cent by volume. Therefore, assuming that only a part of this pore space is drained instantaneously the value of  $f = 0.20$  may be used for drawdown calculations with equation (8). Kirkham and Gaskell also proposed the same value. It may also be assumed that the potential gradients  $\phi_y$  of figure 21 are applicable in the Kirkham-Gaskell analysis, so that the network does not have to be assembled again. The  $\phi_x \tan \theta$  values may again be neglected in the calculations of the initial positions. The results are shown in figure 23 and compared with the results of the analysis proposed in this study.

Two differences can be observed: The water tables obtained with the Kirkham and Gaskell analysis are more curvilinear and the time intervals are longer. As already discussed in the previous paragraph and mentioned by Luthin and Miller, the lag between the water table positions obtained by Kirkham and Gaskell and the experimental ones is due to the omission of the capillary fringe effect. The main difference between the Kirkham and Gaskell equation (8) and equation (15) is the square root form of the latter. As a square root tends to flatten off a function, the water table shapes obtained with equation (15) are considerably flatter. This square root form comes from the linear relationship between the depth of the upper capillary fringe and the apparent drained porosity, which after integration results into the quadratic equation (13) from which equation (15) is derived. Kirkham and Gaskell did not consider a changing drained porosity and consequently did not obtain this square root form in their derivation.

## CONCLUSIONS

1. The assumptions of a completely saturated capillary fringe and of a linear relationship between the porosity factor and the water table depth below the soil surface are validated by the close agreement between predicted and experimental water table drawdown.

2. The Kirkham-Gaskell equation provides a good expression for drawdown calculations provided that it is modified mathematically according to the above assumptions.

3. For practical purposes, such as for wide drain spacings, the generally unknown soil moisture-water table depth relationship can be replaced by the soil moisture-suction relationship. More experimental work is necessary in this respect.

4. The electrical resistance network as described by Worstell and Luthin (1959) is particularly useful for solving saturated flow problems where the potential distribution and the total outflow are required.

5. The proposed method is not very practical for design purposes. It opens new possibilities, however, for further theoretical research. It will serve its main purpose if it is helpful for the evaluation of more practical equations.

### ACKNOWLEDGMENT

The authors are indebted to Mr. R. V. Worstell for the technical advice and help given during the experiment. The study, presented here, was partly supported by funds from W-51, Regional Project on Drainage.

### LIST OF SYMBOLS

The symbols used in the literature review are the ones as used by the original authors (Childs, 1947 and Kirkham-Gaskell, 1951). All the other symbols used in this study are defined in the list below.

- $a$  slope of the soil moisture characteristic curve.
- $f$  fraction of soil volume which is occupied by drainable water.
- $f_a$  average fraction of soil which is occupied by drainable water, or the average drained porosity between two successive positions of the water table.
- $f'$  apparent drained porosity.
- $f'_a$  average apparent drained porosity.
- $f_l$  the fraction of soil volume drained at field capacity.
- $h_c$  height of the upper capillary fringe boundary above the center of the drain.
- $i$  electrical current through entire network.
- $i_0$  electrical current per unit cross sectional area
- $k$  hydraulic conductivity.
- $q$  outflow rate per unit drain length.
- $r_d$  radius of drain pipe.
- $R_0$  basic network resistance or resistivity.
- $s$  distance.
- $T$  time interval ( $\Delta t$ ) between two successive positions of the water table.
- $v$  rate of flow per unit cross sectional area of soil.
- $V$  electrical potential.
- $V_c$  potential of the upper capillary fringe boundary in electrical units.
- $w$  water drained from the entire soil profile above the water table when the water table moves from the  $(n - 1)$ -th to the  $n$ -th position.
- $w'$  water drained from the soil when a stable water table falls from the  $(n - 1)$ -th to the  $n$ -th position.
- $x$  horizontal distance from center of drain.
- $y$  vertical distance below soil surface.
- $y_c$  suction head in the soil at which the capillary fringe is defined.
- $y_n, y_{n-1}$  the average depth of the  $n$ -th and the  $(n - 1)$ -th position of the water table below the soil surface.

- $y'$  depth of the upper boundary of the capillary fringe below the soil surface.  
 $y'_n, y'_{n-1}$  depth of the  $n$ -th and the  $(n - 1)$ -th position of the upper boundary of the capillary fringe below the soil surface.  
 $\theta$  the slope angle of the upper capillary fringe boundary.  
 $\phi$  hydraulic potential.  
 $\phi_c$  hydraulic potential of the upper capillary fringe boundary.  
 $\phi_e$  effective potential gradient defined by  $\phi_y - \phi_x \tan \theta$ .  
 $\phi_x$  horizontal component of the potential gradient obtained just below the upper capillary fringe boundary.  
 $\phi_y$  vertical component of the potential gradient obtained just below the upper capillary fringe boundary.

## LITERATURE CITED

- ARONOVICI, V. S., and W. W. DONNAN  
1946. Soil permeability as a criterion for drainage design. *Amer. Geophys. Union Trans.* **27**:95-101.
- CHILDS, E. C.  
1947. The water table, equipotentials and streamlines in drained land: V. The moving water table. *Soil Sci.* **63**:361-76.
- DAY, PAUL R., and JAMES N. LUTHIN  
1956. A numerical solution of the differential equation of flow for a vertical drainage problem. *Soil Sci. Soc. Amer. Proc.* **20**:443-47.
- DUMM, LEE D.  
1954. New formula for determining depth and spacing of subsurface drains on irrigated lands. *Agr. Engin.* **35**:726-30.
- KIRKHAM, DON, and R. E. GASKELL  
1951. The falling water table in tile and ditch drainage. *Soil Sci. Soc. Amer. Proc.* **15**:37-42.
- LUTHIN, JAMES N.  
1953. An electrical resistance network solving drainage problems. *Soil Sci.* **75**:259-74.  
1959. The falling water table in tile drainage. II. Proposed criteria for spacing tile drains. *Amer. Soc. Agr. Engin. Trans.* **2**:44-45.
- LUTHIN, JAMES N., and R. E. GASKELL  
1950. Numerical solutions for tile drainage of layered soil. *Amer. Geophys. Union Trans.* **31**:595-602.
- LUTHIN, JAMES N., and ROBERT D. MILLER  
1953. Pressure distribution in soil columns draining into the atmosphere. *Soil Sci. Soc. Amer. Proc.* **17**:329-33.
- LUTHIN, JAMES N., and ROBERT V. WORSTELL  
1957. The falling water table in tile drainage—A laboratory study. *Soil Sci. Soc. Amer. Proc.* **21**:580-84.
- MUSKAT, M.  
1946. Flow of homogeneous fluids through porous media. J. W. Edwards, Ann Arbor, Mich., 763 pp.
- SPÖTTLE, J.  
1911. Landwirtschaftliche Bodenverbesserungen, Handb. d. Ingen. Wiss., Part 3, Der Wasserbau, 4th ed. Wilhelm Engelmann, Leipzig, 7:1-470.
- VISSER, W. C.  
1953. De grondslagen van de drainage berekening. *Landbouwk. Tijdschr.* **65**:66-81.
- WALKER, PHELPS  
1952. Depth and spacing for drain laterals as computed from core-sample permeability measurements. *Agr. Engin.* **33**:71-73.
- WORSTELL, ROBERT V., and JAMES N. LUTHIN  
1959. A resistance network analog for studying seepage problems. *Soil Sci.* **88**:267-69.



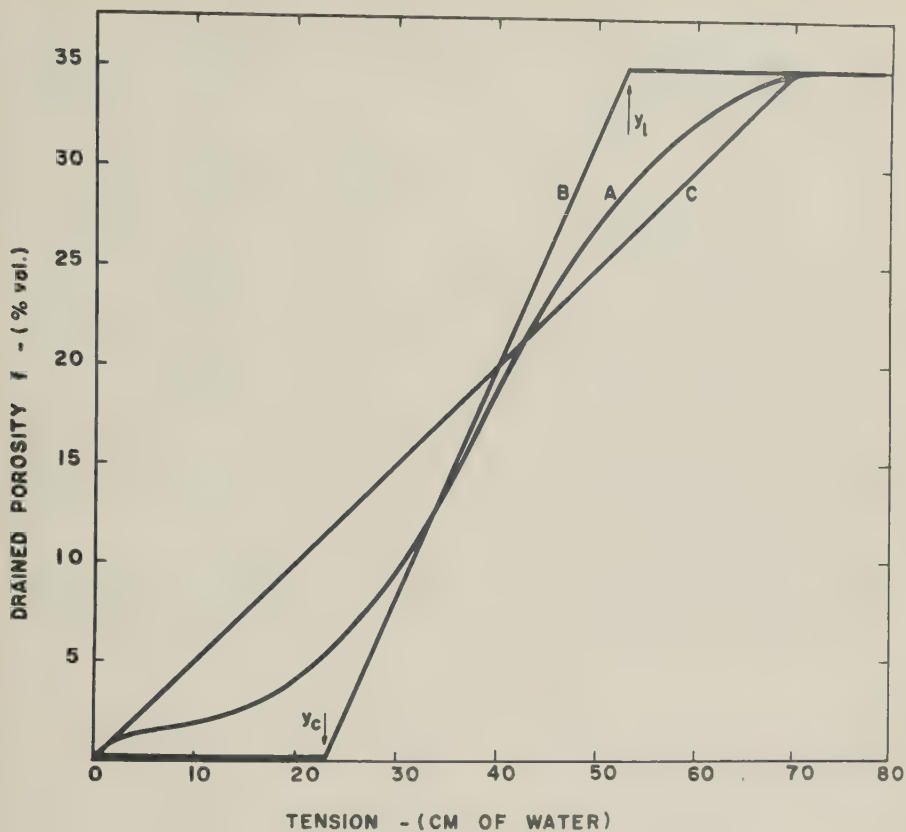


Fig. 2. Soil moisture-suction relationship for Oso Flaco sand.

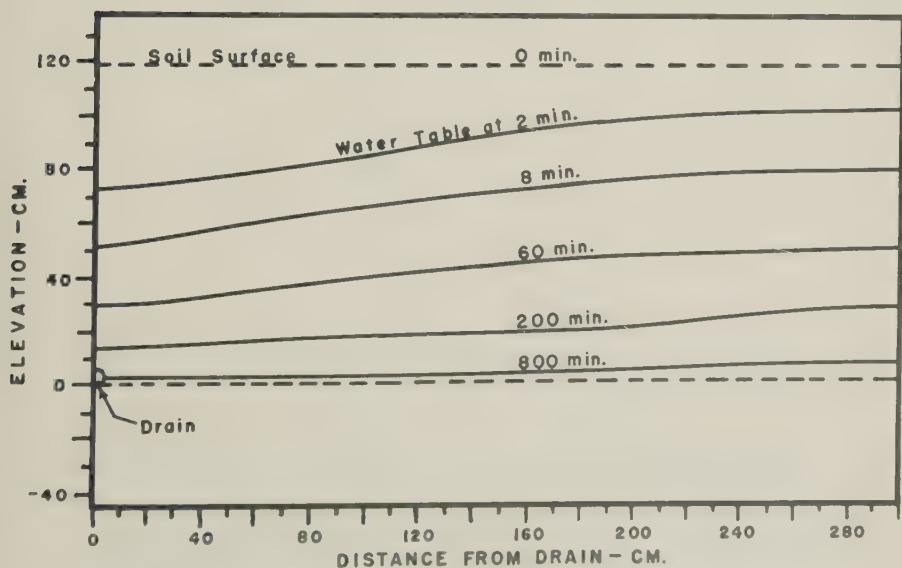


Fig. 3. Successive positions of the water table as obtained experimentally by Luthin and Worstell (1957).

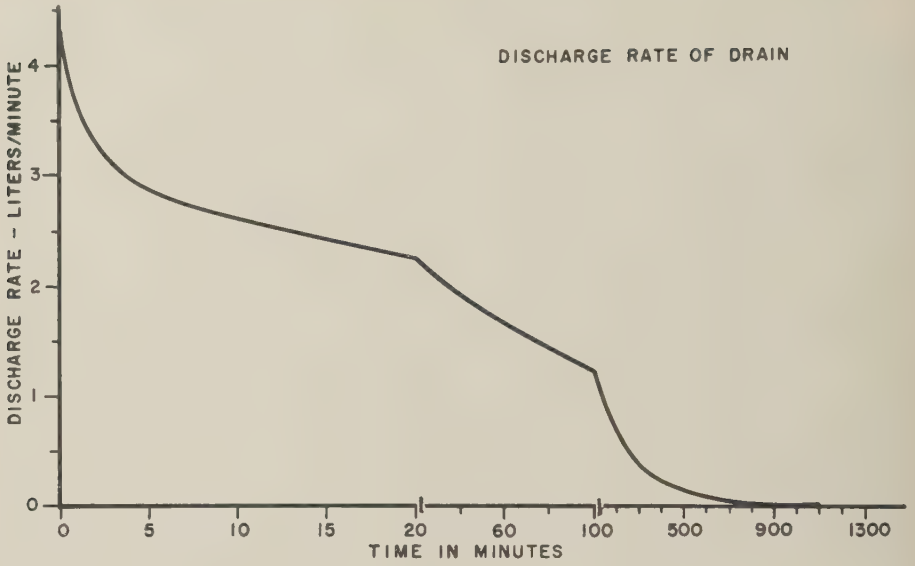


Fig. 4. Drain outflow rate as obtained by Luthin and Worstell (1957).

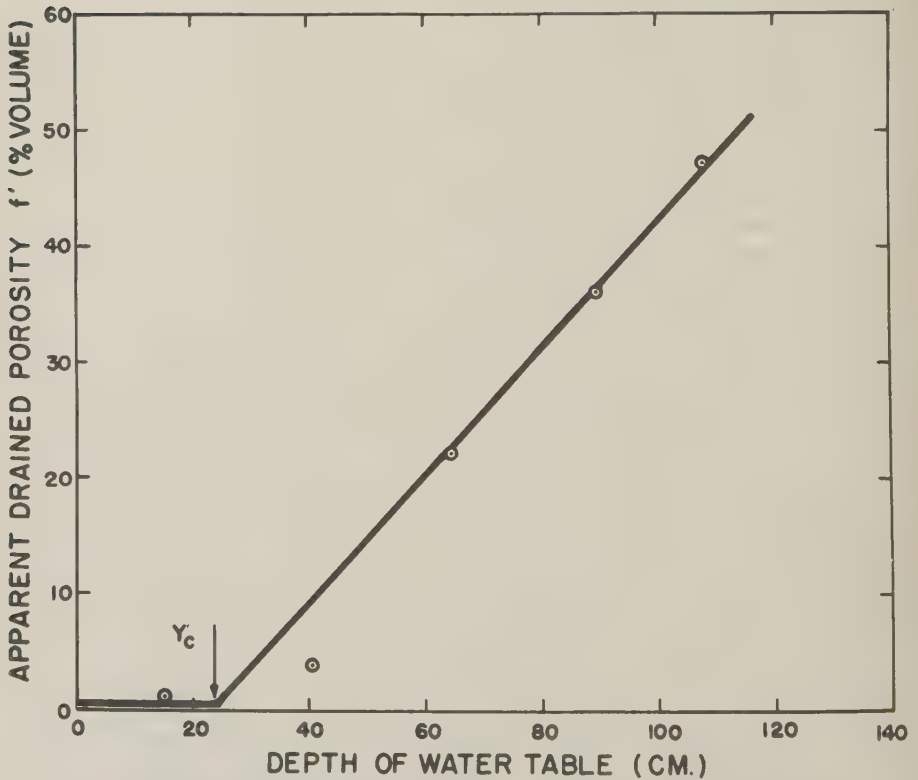


Fig. 5. Soil moisture-water table depth relationship during drainage of model tank of Luthin and Worstell.

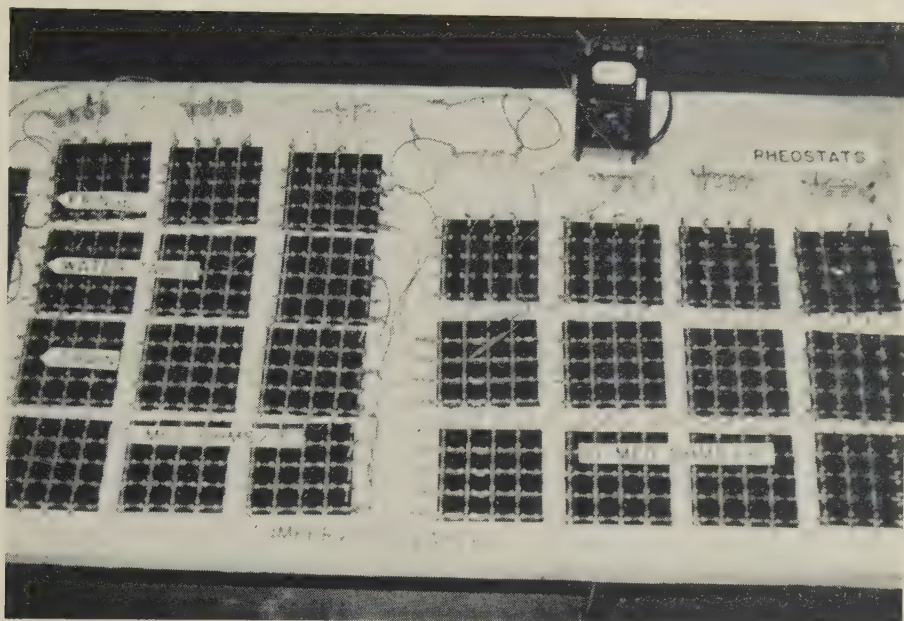


Fig. 6. General view of the electrical resistance network as assembled to simulate "position 5" (see text).

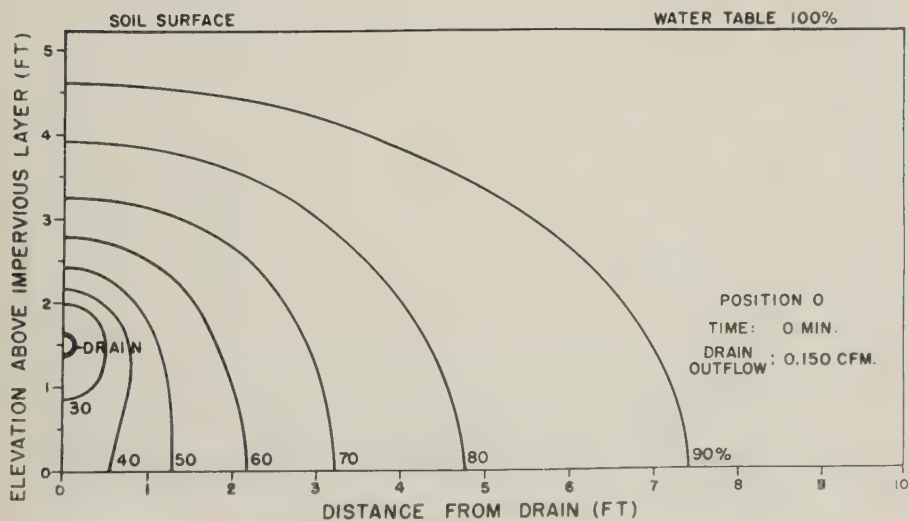


Fig. 7. Illustration of the potential distribution in the soil for the ponded water condition as determined with the electrical resistance network.

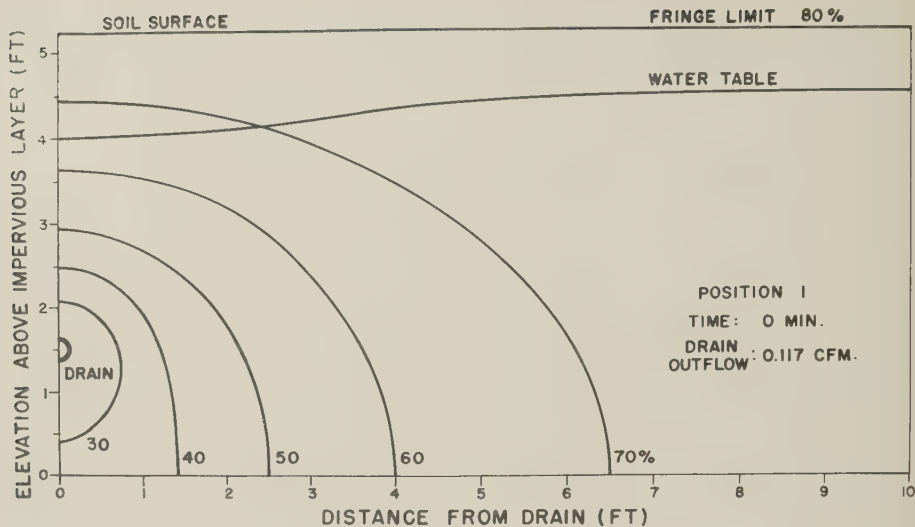


Fig. 8. Illustration of the potential distribution in the soil for position 1 of the water table. The upper boundary of the capillary fringe is at the soil surface.

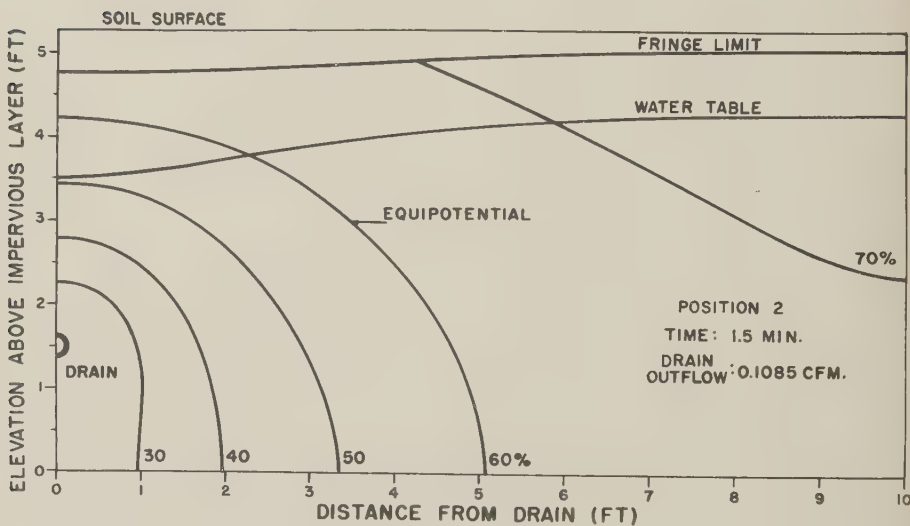


Fig. 9. Illustration of the potential distribution in the soil for position 2 of the water table.

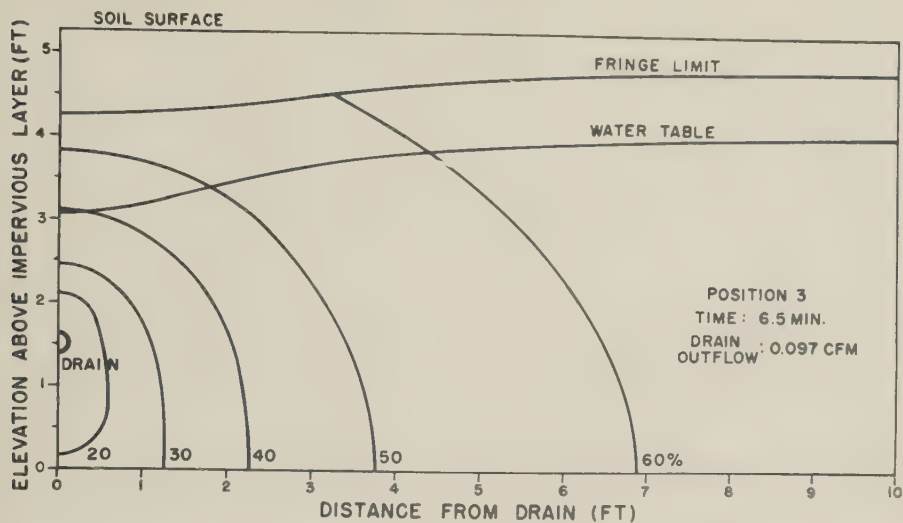


Fig. 10. Illustration of the potential distribution in the soil for position 3 of the water table.

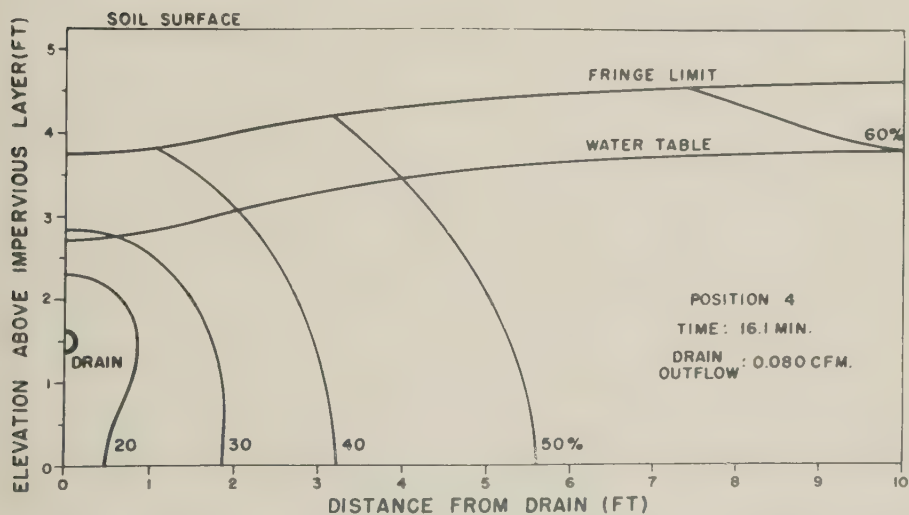


Fig. 11. Illustration of the potential distribution in the soil for position 4 of the water table.

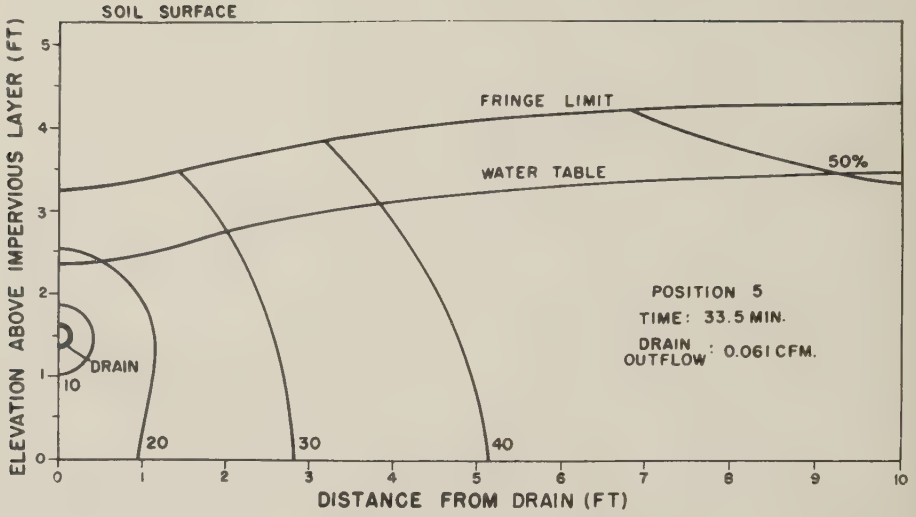


Fig. 12. Illustration of the potential distribution in the soil for position 5 of the water table.

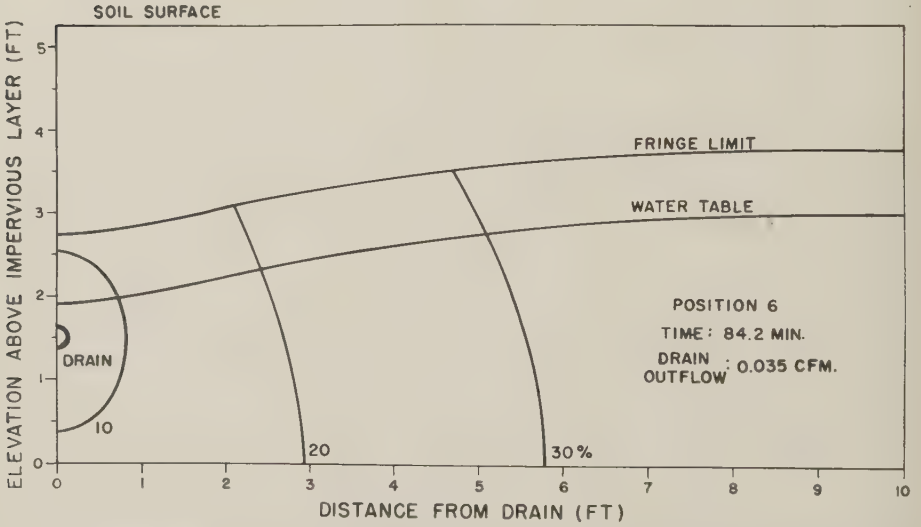


Fig. 13. Illustration of the potential distribution in the soil for position 6 of the water table.

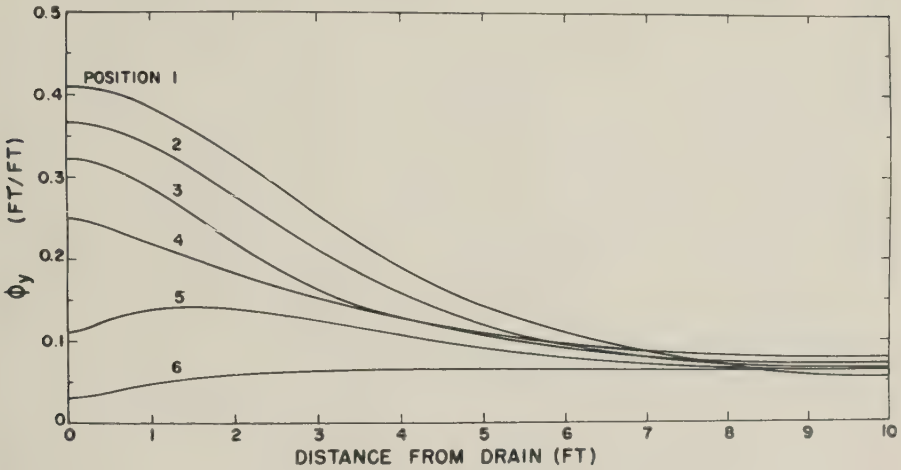


Fig. 14. Vertical components of the potential gradient ( $\phi_y$ ) at the upper capillary fringe boundary.

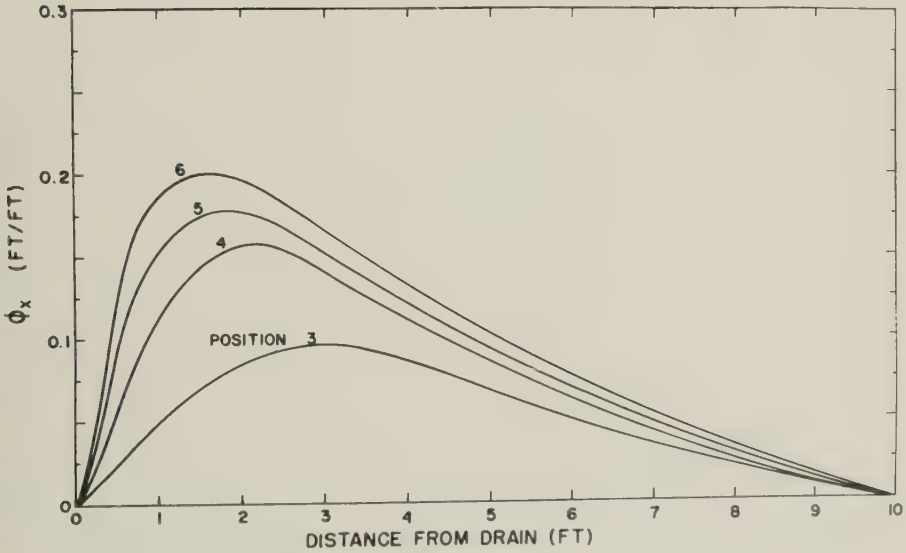


Fig. 15. Horizontal components of the potential gradients ( $\phi_x$ ) at the upper capillary fringe boundary.

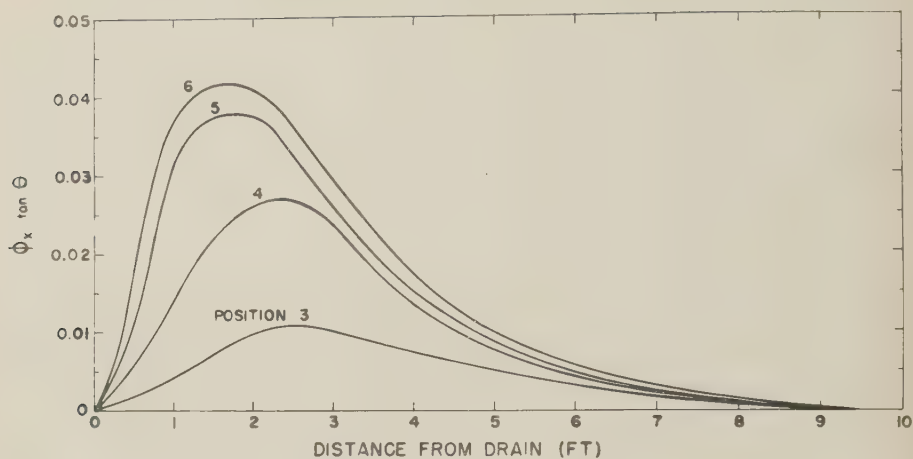


Fig. 16. Curves showing the increasing values of the product ( $\phi_x \tan \theta$ ) as the water table recedes.

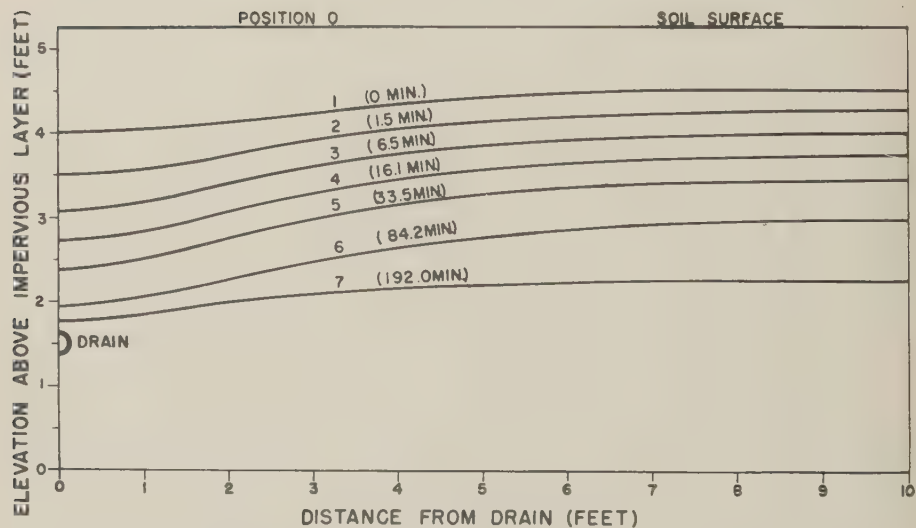


Fig. 17. Successive positions of the water table as obtained by using equation (15).

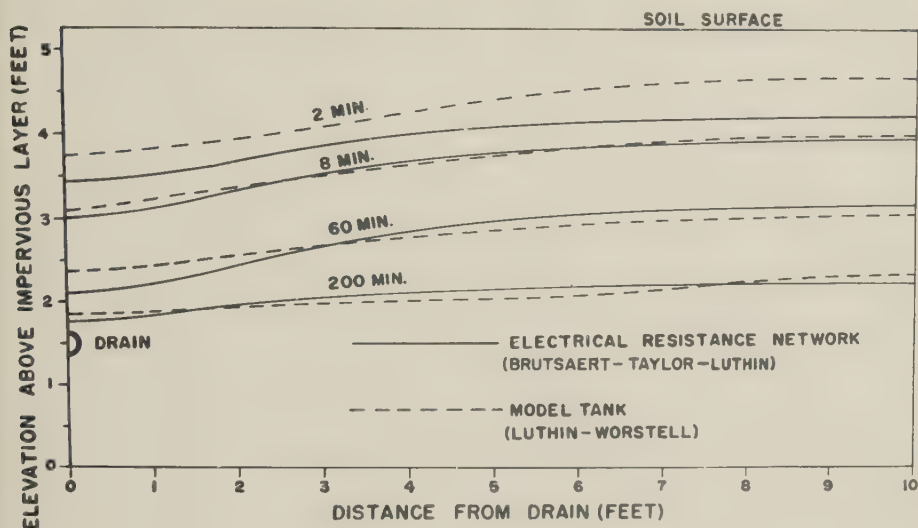


Fig. 18. Water table positions as determined by equation (15) and those obtained experimentally by Luthin and Worstell (1957).

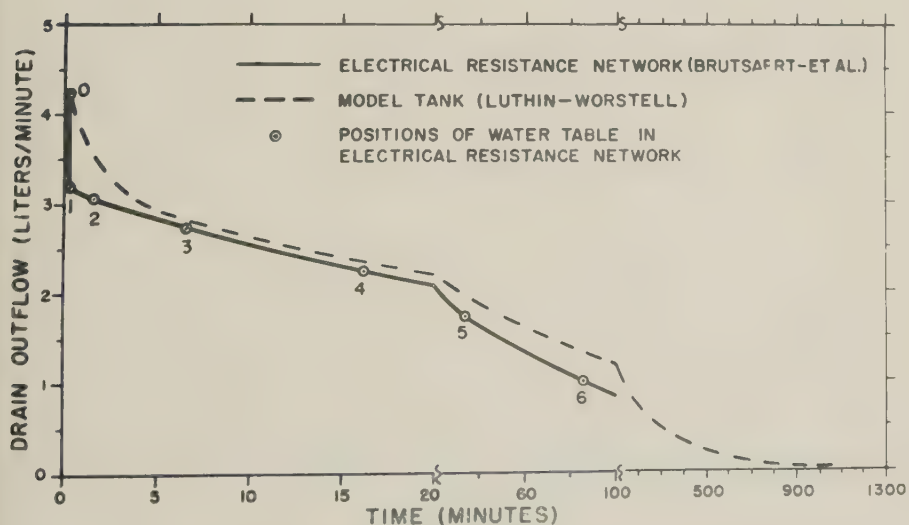


Fig. 19. Comparison between the drain outflow rates, as determined experimentally with a tank model and those predicted by drawdown analysis.

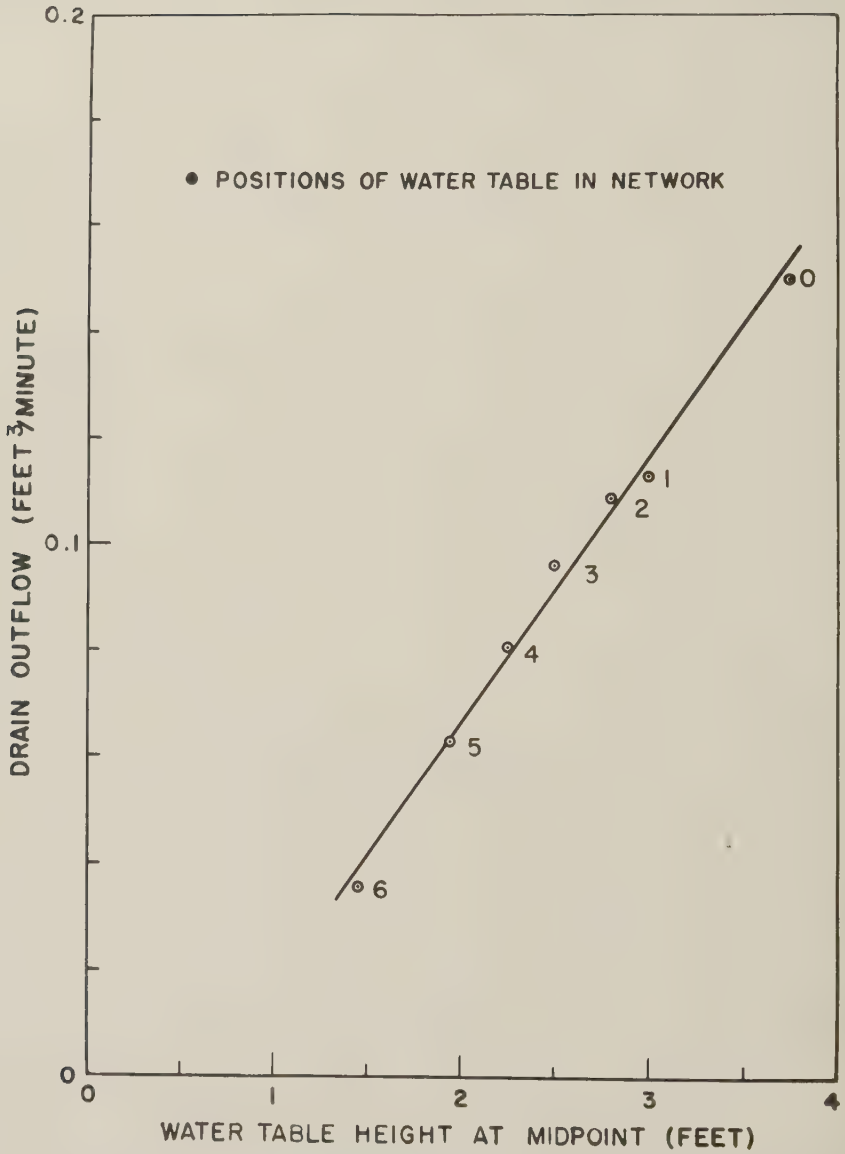


Fig. 20. Relationship between the water table height at the midpoint and the rate of flow from the drain.

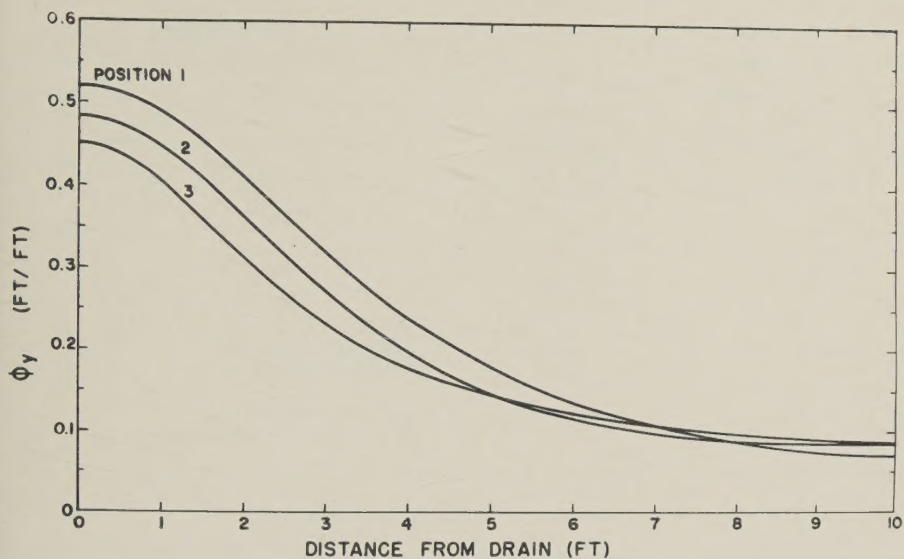


Fig. 21. Vertical components of the potential gradients  $\phi_y$  at the water table when the capillary fringe is neglected.

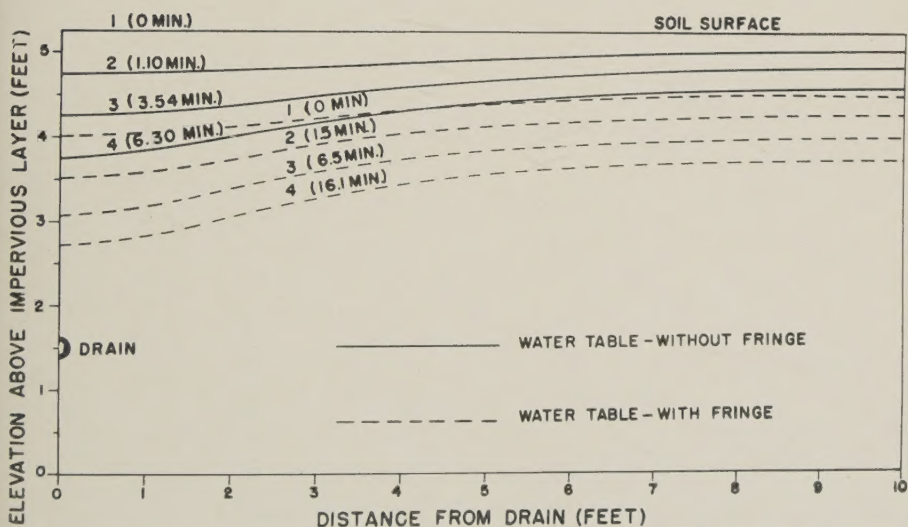


Fig. 22. Comparison between the water table positions with and without capillary fringe.

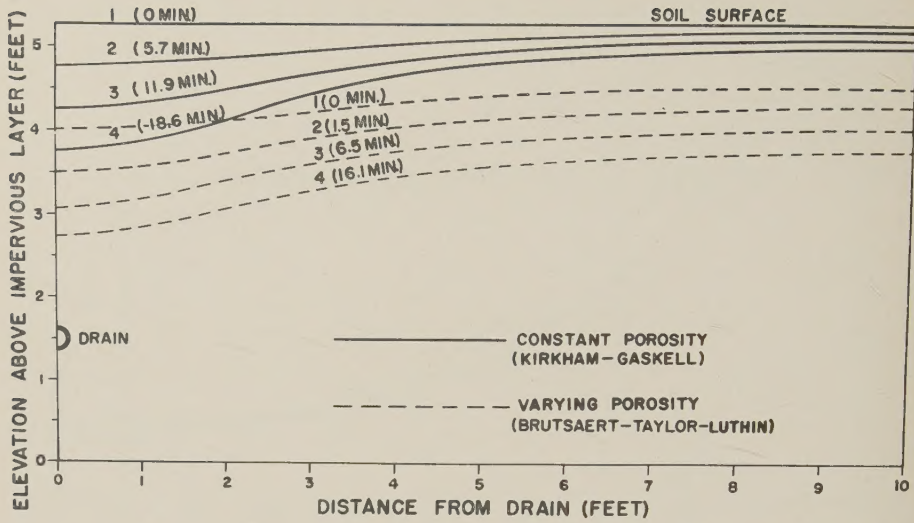


Fig. 23. Comparison of the water table positions obtained by the Kirkham-Gaskell (1951) method with those obtained in this study.



